On the nucleation of creep and the interaction between creep and seismic slip on rate- and state-dependent faults

Alon Ziv[1]

[1] Previous studies of rupture nucleation were restricted to conditions well within the unstable regime. In this study, we show that positive stress changes applied on intrinsically stable interfaces can trigger quasi-static slip episodes. Similar to the onset of ruptures on unstable fractures, the creep on intrinsically stable fractures too are preceded by intervals during which the slip is highly localized. The size of the nucleation patch depends not only on the constitutive parameters, but also on the stressing history. We examine the effect of a stress step on the slip history of a seismic fault interacting with a creeping segment, and show that stress transfer due to creep may strongly affect the timing of an impending seismic slip. Finally, we investigate the effect of a stress step on the slip history of an isolated unstable strip surrounded by creep, and show that a positive stress step triggers aftershocks, whose rate decays as 1/time during most of the sequence, but much faster than 1/time shortly after the stress step. **Citation:** Ziv, A. (2007), On the nucleation of creep and the interaction between creep and seismic slip on rate- and state-dependent faults, *Geophys. Res. Lett.*, *34*, L15303, doi:10.1029/2007GL030337.

1. Introduction

[2] We investigate the onset of creep events, and examine consequences of interaction between creep and seismic slip in the context of the rate- and state-dependent friction. According to friction experiments, the coefficient of friction is a logarithmic function of the slip rate, $\dot{\delta}$, and the contact state, θ, as [*Dieterich*, 1979; *Ruina*, 1983]:

$$\mu = \mu^{\infty} + a\ln(\dot{\delta}/\dot{\delta}^{\infty}) + b\ln(\theta\dot{\delta}^{\infty}/D_c), \quad (1)$$

where μ^{∞} is the steady-state friction when the contact slips at the reference speed, $\dot{\delta}^{\infty}$, a and b are constitutive parameters, and D_c is a characteristic slip distance. The state evolves with both slip and time, and experimental data may be reasonably fit with [*Ruina*, 1980]:

$$d\theta/dt = 1 - \theta\dot{\delta}/D_c. \quad (2)$$

When at steady-state, $\theta = D_c/\dot{\delta}$ and:

$$\mu = \mu^{\infty} + (a-b)\ln\left(\dot{\delta}/\dot{\delta}^{\infty}\right) = \mu^{\infty} + (b-a)\ln\left(\theta\dot{\delta}^{\infty}/D_c\right). \quad (3)$$

[1]Department of Geological and Environmental Sciences, Ben-Gurion University of the Negev, Beer-Sheva, Israel.

Thus, steady-state friction is velocity weakening if $a/b < 1$, and velocity strengthening if $a/b > 1$. While the first situation favors unstable slip, the latter favors creep and is said to be intrinsically stable [*Marone and Scholz*, 1988]. Scientists have long been seeking to understand how earthquakes begin. Previous studies that employed (1)–(2) showed that ruptures are preceded by intervals during which slip is highly localized [*Dieterich*, 1992; *Rice*, 1993; *Rubin and Ampuero*, 2005]. These investigations were restricted to conditions well within the inherently unstable regime. In the first part of this study (section 3) we model slip localization within the intrinsically stable regime. We shall see that, similar to seismic ruptures, creep events too develop from a well defined area over which slip localization takes place.

[3] In the second part of this paper (section 4), we investigate consequences of interaction between seismic slip and creep. Specifically, we examine the effect of a stress step on the rupture time of a seismic segment adjacent to a creeping segment, and simulate the slip history resulting from a stress step applied on a brittle patch surrounded by an otherwise creeping fault. The results of this study have important implications for the physics of slow earthquakes, and for time-dependent earthquake hazard assessments on seismic faults that are located in the vicinity of creeping segments. Next, we describe the model.

2. Modeling Slip on a Fault Governed by Rate- and State-Dependent Friction

[4] An in-plane fracture is represented by an array of n infinitely long dislocations. When modeling multiple ruptures, it is useful to add a seismic radiation term to the stress balance equation (as in *Rice* [1993]). The radiation damping term is representative of the outflow of energy due to seismic waves, and it's incorporation ensures that the slip rate remain finite at all times. For the modeling of the localization stage, on the other hand, both quasi-dynamic and quasi-static approaches are appropriate. In section 3, we wish to compare the dimensions of the localization patch with predicted dimensions for quasi-static crack, therefore we adopt a quasi-static approach. In section 4, on the other hand, we model multiple cycles and therefore use a quasi-dynamic approach. We write the stress balance equation as:

$$\sigma\left[\mu^{\infty} + a\ln(\dot{\delta}_i/\dot{\delta}^{\infty}) + b\ln(\theta_i\dot{\delta}^{\infty}/D_c)\right] = \tau_0 + \dot{\tau}_i^{\infty}t + \sum_{j=1}^{n} g_{ij}\delta_j$$
$$- \delta_{QD}(G/2\beta)d\dot{\delta}_i/dt, \quad (4)$$

where the subscripts are dislocation indexes, σ is the normal stress, τ^0 is a constant, $\dot{\tau}^{\infty}$ is the remote stressing rate, g_{ij} is

an elasto-static kernel, δ is the slip, G is the shear modulus, β is the shear wave speed, and δ_{QD} is set to be equal to 1 when taking a quasi-dynamic approach, and is set to 0 otherwise. The state on i evolves as:

$$d\theta_i/dt = 1 - \theta_i\dot{\delta}_i/D_c \qquad (5)$$

For a crack whose long-term slip rate is equal to $\dot{\delta}^\infty$, the long-term stressing rate is equal to:

$$\dot{\tau}_i^\infty = -\sum_{j=1}^{n} g_{ij}\dot{\delta}^\infty \qquad (6)$$

Replacing (6) in (4), and solving for $d\dot{\delta}_i/dt$ gives:

$$d\dot{\delta}_i/dt = \frac{\sum_{j=1}^{n} g_{ij}(\dot{\delta}_j - \dot{\delta}^\infty) - (b\sigma/\theta_i)d\theta_i/dt}{a\sigma/\dot{\delta}_i + \delta_{QD}G/2\beta} \qquad (7)$$

Equations (5) and (7) are integrated numerically using an adaptive time-stepping algorithm.

[5] The elastic kernel is wrapped around, resulting in a periodic boundary conditions with a wavelength that is equal to n. The kernel is calculated using equations 32–33 of *Dieterich* [1992], with a shear modulus and a Poisson's ratio that are equal to 10 GPa and 0.25, respectively. The convolution theorem is implemented to calculate the elastic interaction term (i.e., the sum over $g_{ij}(\dot{\delta}_j - \dot{\delta}^\infty)$). This is done using the FFTW library (www.fftw.org), which unlike conventional FFT algorithm can transform data of any length. The fault is represented by 2×10^4 dislocations, each of which is 0.05 m long. The model parameters that are identical in all calculations are: $a = 0.02$, $D_c = 0.001$ m, $\dot{\delta}^\infty = 3 \times 10^{-9}$ m/s (corresponding to 10 centimeters per year) and $\sigma = 100$ MPa. In quasi-dynamic calculations we use: $\beta = 3000$ m/s. We carried out calculations with various a and b (detailed below), and verified that the localization patch is well resolved in all calculations.

3. Creep Localization Resulting From a Positive Stress Change

[6] Spontaneous onset of creep events is possible if the spatial distribution of the constitutive parameters a and $(a - b)$ is heterogeneous [*Liu and Rice*, 2005]. In homogeneous models, however, slip episodes on velocity-strengthening segments are only possible if the system is externally perturbed. The stress perturbations that we apply are position dependent and are given by:

$$\Delta\bar{\tau}_i = \Delta\bar{\tau}_{\min} + (\Delta\bar{\tau}_{\max} - \Delta\bar{\tau}_{\min})\sin(\pi i/n), \qquad (8)$$

where $\Delta\bar{\tau}_{\min}$ and $\Delta\bar{\tau}_{\max}$ are minimum and maximum stress perturbations, respectively, and the bars indicate normalization by $a\sigma$. Perturbing the stress in such a way is convenient, since it forces the nucleation to take place at the model's center.

[7] Starting from steady-state, we impose an instantaneous stress step whose $\Delta\bar{\tau}_{\min}$ and $\Delta\bar{\tau}_{\max}$ are equal to 3 and 4, respectively. In that case, since the sliding speed after the

stress perturbation is much larger than that during steady-state, the second term on the right-hand side of (5) is much larger than a unity. Thus, $d\theta/dt \approx -\theta\dot{\delta}/D_c$ and θ decreases with slip proportionally to $\exp(-\delta/D_c)$ [*Dieterich*, 1992]. *Dieterich* [1992] pointed out that this approximation is valid to the extent that the sliding speed increase overwhelm the effect of state decrease, and following *Rubin and Ampuero* [2005] we refer to it as the "no-healing" approximation.

[8] Profiles of θ and $\dot{\delta}$ at successive times during slip localization are shown in Figures 1a–1b and 1c–1d for $a/b = 0.9$ and $a/b = 1.1$, respectively. Indeed, in both cases the state drops, and this drop is accompanied by sliding speed increase. Note that in either case the slip is highly localized, and the area undergoing rapid slip defines the localization patch. Despite the apparent similarities in the rate and state profiles for $a/b = 0.9$ and $a/b = 1.1$, the evolution of the two systems is quite different. To see that it is useful to examine the evolution of $d\theta/dt$ (Figures 1c and 1f). In either case, because the model is subjected to a positive stress change, the sign of $d\theta/dt$ is negative and the contact surface is undergoing weakening. For $a/b = 0.9$, $d\theta/dt$ initially decreases, i.e. the contact surface is undergoing weakening at an increasing rate. Only at a later stage during the localization does $d\theta/dt$ within the slipping patch increase. For $a/b = 1.1$, on the other hand, $d\theta/dt$ increases for all times, and the rate at which it increases is larger inside the localization patch than elsewhere. The localization phase, often referred to as the nucleation phase, is followed by a propagation phase, during which the crack is expanding. The propagation is quasi-static if $a/b > 1$, and since in this calculation $\delta_{QD} = 0$, sliding speed is unbounded if $a/b < 1$.

[9] From (7), the condition for slip acceleration (i.e., $d\dot{\delta}/dt > 0$) is:

$$\sum_{j=1}^{n} g_{ij}(\dot{\delta}_j - \dot{\delta}^\infty) > (b\sigma/\theta_i)d\theta_i/dt. \qquad (9)$$

Similarly, for a crack of length L embedded within an elastic medium whose shear modulus is G, one can write:

$$(-\eta G/L)(\dot{\delta} - \dot{\delta}^\infty) > (b\sigma/\theta)d\theta/dt, \qquad (10)$$

where η is a geometrical constant with a value that is close to a unity. Neglecting remote stressing, and replacing $d\theta/dt$ with it's "no-healing" approximation, $-\dot{\delta}\theta/D_c$, leads to:

$$L > \eta GD_c/b\sigma \equiv L_D, \qquad (11)$$

where L_D is *Dieterich*'s prediction for the size of the localization patch. Thus, according to *Dieterich* [1992] the size of the localization patch depends on b and D_c, but not on a.

[10] As given by *Rubin and Ampuero* [2005], the size of the patch is obtained by calculating the distance between the peaks in the elastic stress profiles (i.e., equation (4)). The localization patch size, $L_{\min}$, is simply the minimum time-dependent patch length. In Figure 2 we show $L_{\min}/L_D$ as a function of a/b for various stress steps. Note that the size of the localization patch depends not only on b, but also on a/b and the magnitude of the stress application. Note that
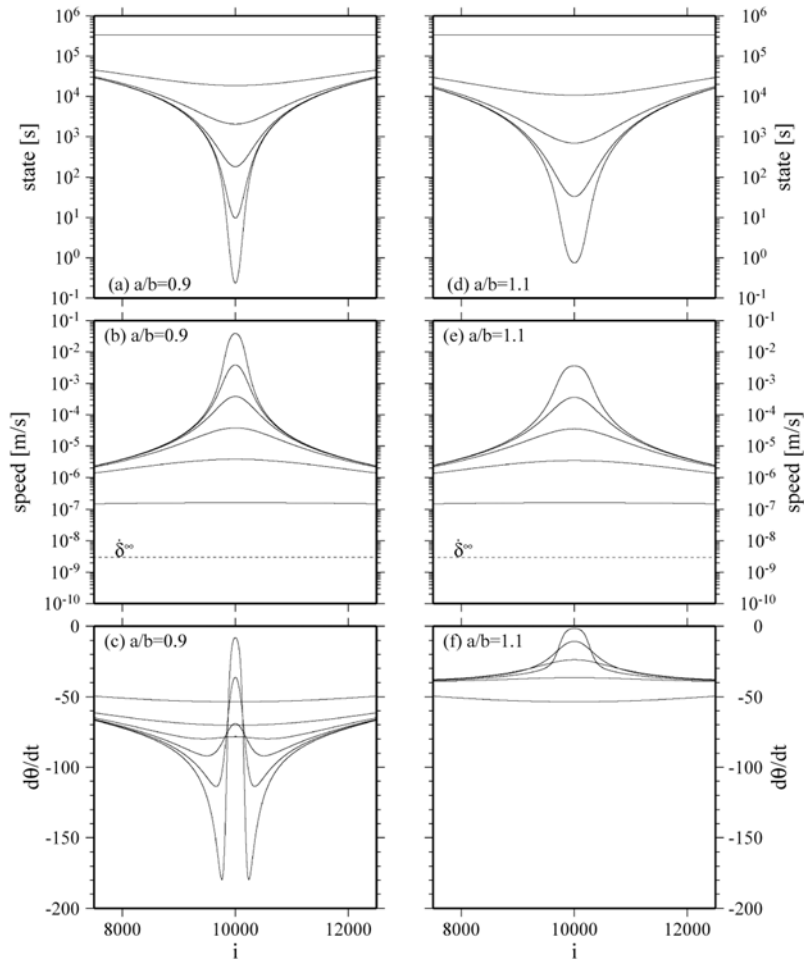
Figure 1. Comparison between the evolution of contact state, sliding speed, and $d\theta/dt$ during slip localization for (a, b, c) $a/b = 0.9$ and (d, e, f) $a/b = 1.1$. The dashed lines in Figures 1b and 1e denote the remote sliding speed, $\dot{\delta}^\infty$. A contour is drawn each time a 10-fold increase in the maximum sliding speed is seen.

$L_{min} \geq 1.37 \, L_D$, and that L_{min} approaches $1.37 \, L_D$ for increasing $\Delta\bar{\tau}$ and decreasing values of a/b. The effect of the stress steps is easy to understand; larger positive stress perturbations push the fault further above the steady-state, keeping the ''no-healing'' approximation valid for longer times and bringing L_{min} closer to L_D.

[11] Interestingly, negative stress changes too may trigger creep events. Similar to creep events triggered by positive stress perturbations, they too are preceded by accelerating slip within a localization patch, whose size depends on the magnitude of the stress perturbation (J.-P. Ampuero and H. Perfettini, manuscript in preparation, 2007).

4. Interaction Between Creep and Seismic Slip

4.1. Why Should Interaction With Creep Be Accounted for in Hazard Analyses?

[12] To simulate the effect of a stress step on the slip history of a seismic fault interacting with a creeping segment, we set $a/b = 0.9$ for $1 \leq i \leq 10^4$, and set $a/b = 1.1$ for $10^4 < i \leq 2 \times 10^4$. The distribution of the slip rate and contact state in such a system is never uniform. In order to obtain physically sensible initial conditions, it is necessary to evolve the simulation through several stick-slip

cycles so that the system spontaneously reaches to its limit circle. For that reason we switch to a quasi-dynamic scheme, i.e. we set δ_{QD} in (7) to be equal to 1. As in previous quasi-dynamic continuous models that incorporate
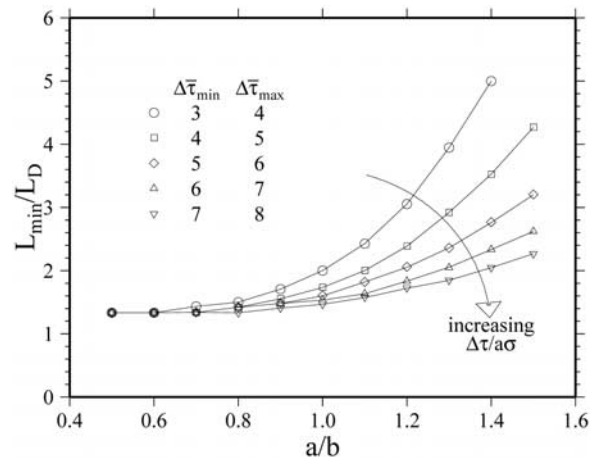
Figure 2. A plot of L_{min}/L_D as a function of a/b for various stress steps.
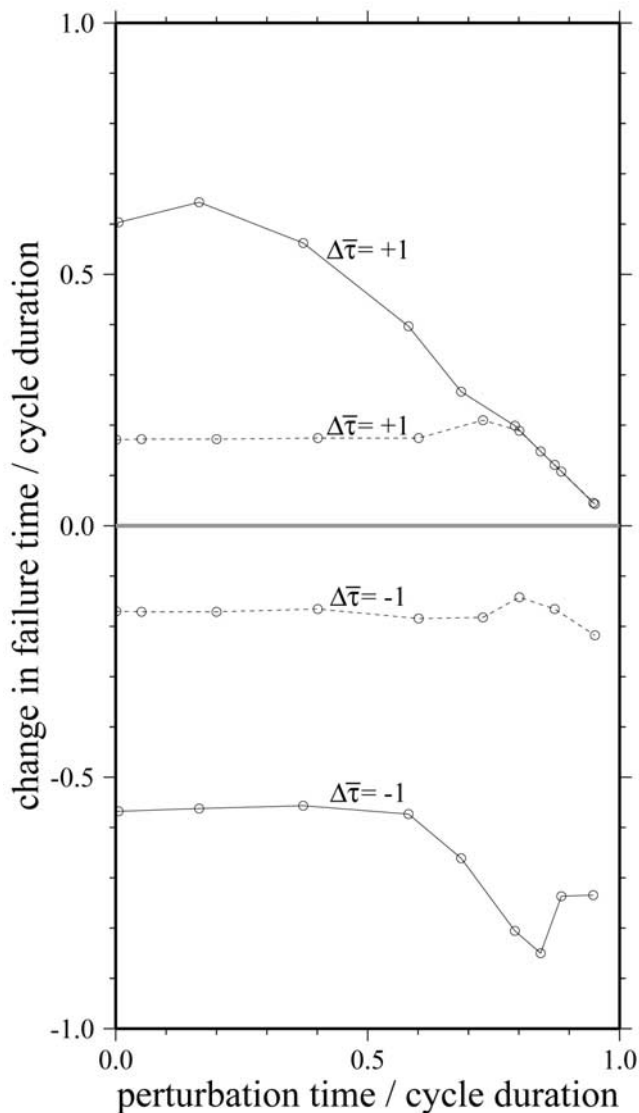
Figure 3. The change in failure time caused by uniform stress steps of $\Delta\bar{\tau} = +1$ and $\Delta\bar{\tau} = -1$ as a function of the time of the stress application, with both axes being normalized by the duration of the unperturbed cycle, and the time of the stress application measured since the previous slip episode. Models incorporating velocity strengthening and steady slip are indicated by solid and dashed lines, respectively.

rate- and state-dependent creep and stick-slip [*Tse and Rice,* 1986; *Rice,* 1993], the model soon produces periodic repetition of stick-slip cycles. The initial conditions that we use are snapshots of the rate and state distribution at various stages of the seismic cycle. To assess the extent to which interaction with creep is important, we compare the results of this model with that of a model in which the boundary condition on $10^4 < i \le 2 \times 10^4$ is replaced by a constant slip rate of $\dot{\delta}^{\infty}$. The duration of the seismic cycle in the model incorporating creep is nearly equal to that in which creep is replaced by steady slip.

[13] The changes in the failure time caused by uniform positive and negative stress steps are shown in Figure 3 as a function of the time of the stress application (with both axes being normalized by the duration of the unperturbed cycle). As expected, while positive stress changes advance the failure time, negative stress steps delay the rupture. Additionally, the amount of time advance and time delay is a function of when in the cycle the stress is imposed [*Dieterich,* 1994; *Gomberg et al.,* 1998]. The result that we wish to emphasis here is that interaction with creep may strongly affect the amount of time advance and delay. Specifically, in this example, the time advance and delay may be significantly larger if the seismic segment is interacting with rate- and state-dependent creep rather than with steady slip. This has important implications for time-dependent earthquake hazard assessments on faults that are located in the vicinity of creeping segments. For example, the stress change that the 1983 Coalinga-Nuñez earthquakes induced on the San Andreas fault may have affected the timing of the Parkfield earthquake [*Toda and Stein,* 2002]. In the light of our findings, it is very important that the stress transfer from the creeping section to the north of the Parkfield segment be also taken into account when assessing the response of the Parkfield segment to the Coalinga-Nuñez quakes.

4.2. On the 1/time Decay of Repeating Aftershocks

[14] How may the 1/time decay of repeating aftershocks arise from interaction with creep? *Vidale et al.* [1994] suggested that repeating earthquakes are occurring on brittle patches that are embedded within an otherwise creeping fault. In that case, the stressing rate acting on the brittle patches, and therefore also the recurrence interval of repeating ruptures are directly proportional to the creep rate (assuming ruptures are of constant stress drop). Thus, 1/time decay of repeating aftershocks is expected if the creep rate is inversely proportional to time. Differentiating (3) with respect to time suggests that the creep rate may indeed vary as 1/time [*Schaff et al.,* 1998]. This argument, however, rests on the assumption that the conditions on the creeping segment are close to steady-state. This may be true during most of the aftershock sequence, but it is certainly not true shortly after a stress perturbation. Because it is not evident when and for how long the steady-state assumption is valid, it is instructive to investigate this model numerically.

[15] To simulate the effect of a stress step on the slip history of an isolated unstable patch trapped within a creeping fault, we set a/b to 1.1, except within a small region that is 50 meters long (i.e., 1000 dislocations) at the center of the model, where we set a/b to 0.9. Since the objective here is to model repeating ruptures, we use aquasi-dynamic approach. In Figures 4a and 4b we show the evolution of slip resulting from a uniform stress step of $\Delta\bar{\tau} = 1$ applied 10% and 90% into the seismic cycle, respectively. Early in the cycle, i.e. shortly after a co-seismic slip, the velocity strengthening area near the brittle patch is highly stressed and is closer to failure than the velocity strengthening area far from the brittle patch. For that reason, the creep event nucleates close to the brittle patch if the stress is perturbed early in the cycle, and nucleates far from the brittle patch if the system is perturbed near the cycle end.
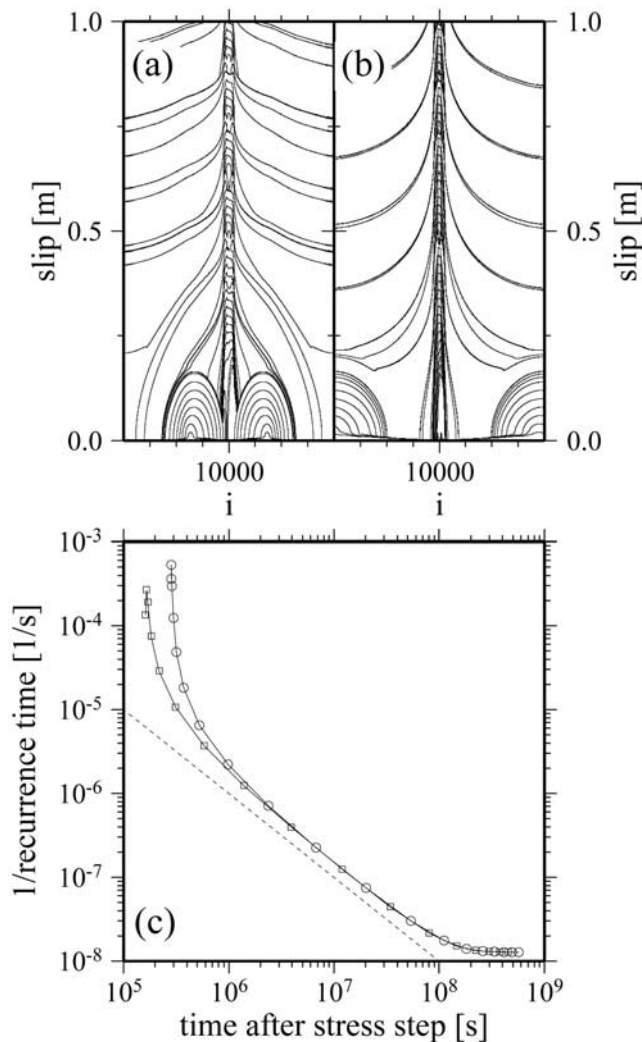
Figure 4. (a, b) Profiles of slip following a uniform stress step of $\Delta\bar{\tau} = 1$. A contour is drawn each time the maximum cumulative slip increases by 2 centimeters with respect to the previous contour. The slip history shown here is for the first five aftershocks, corresponding to an interval that is less than 3×10^5 seconds since the stress application. In Figures 4a and 4b the stress is applied 10% and 90% into the seismic cycle, respectively. (c) The inverse of the rupture recurrence times as a function of time since the stress step. The circles and the squares correspond to Figures 4a and 4b, respectively. The dashed line indicates a decay rate of 1/time.

[16] The inverse of the rupture recurrence times as a function of time since the stress step are shown in Figure 4c. Indeed, during most of the aftershock activity (between 10^6 and 10^8 seconds) the rupture rate decays asymptotic to 1/time. For times less than 10^6 seconds, however, since the state of stress is well above the steady-state, the decay of the creep rate, and therefore also the failure rate exceeds notably the 1/time curve. To the best of our knowledge, such a transition in the decay rate of repeating quakes has not been reported.

[17] Finally, it is interesting to compare the magnitude of the seismicity rate change emerging from this model with that predicted by Dieterich's aftershock model [*Dieterich*, 1994]. While according to Dieterich's model a stress step of $1\sigma a$ results in an e-fold increase in the seismicity rate, the seismicity rate here increased by more than 4 orders of magnitude. Thus, the mechanism suggested by *Schaff et al.* [1998] is a very efficient one, in the sense that a modest stress perturbation may give rise to a large increase in earthquake production rate.

5. Conclusions

[18] We model slip nucleation on rate- and state-dependent fault, and show that positive stress changes applied on conditionally stable fractures can trigger quasi-static slip episodes. Similar to the onset of ruptures on inherently unstable fractures, the creep on conditionally stable fractures too are preceded by intervals during which the slip is highly localized. The size of the localization patch depends on the constitutive parameters a/b, D_c, as well as on the stressing history. Specifically, $L_{\min} \geq 1.37\ L_D$, and $L_{\min}$ approaches $1.37\ L_D$ for increasing $\Delta\bar{\tau}$ and decreasing values of a/b.

[19] We examine the effect of a stress step on the slip history of a seismic fault interacting with a creeping segment. We show that stress transfer due to creep may strongly affect the timing of an impending seismic slip. This has important implications for time-dependent earthquake hazard assessments on faults that are interacting significantly with aseismic segments.

[20] We model slip on an isolated brittle patch trapped within a creeping fault. We show that the effect of a positive stress step is to increase the rate of repeating earthquakes. The decay of aftershock rate is asymptotic to 1/time during most of the aftershock activity, but is much faster than 1/time, shortly after the stress step when the state of stress on the creeping portion of the model is well above steady-state.

References

Dieterich, J. H. (1979), Modeling of rock friction: 1. Experimental results and constitutive equations, *J. Geophys. Res.*, *84*, 2161–2168.

Dieterich, J. H. (1992), Earthquake nucleation on faults with rate- and state-dependent strength, *Tectonophysics*, *211*, 115–134.

Dieterich, J. (1994), A constitutive law for rate of earthquake production and its application to earthquake clustering, *J. Geophys. Res.*, *99*, 2601–2618.

Gomberg, J., N. M. Beeler, M. L. Blanpied, and P. Bodin (1998), Earthquake triggering by transient and static deformations, *J. Geophys. Res.*, *103*, 24,411–24,426, doi:10.1029/98JB01125.

Liu, Y., and J. R. Rice (2005), Aseismic slip transients emerge spontaneously in three-dimensional rate and state modeling of subduction earthquake sequences, *J. Geophys. Res.*, *110*, B08307, doi:10.1029/2004JB003424.

Marone, C., and C. Scholz (1988), The depth of seismic faulting and the upper transition from stable to unstable slip regimes, *Geophys. Res. Lett.*, *15*, 621–624.

Rice, J. R. (1993), Spatio-temporal complexity of slip on a fault, *J. Geophys. Res.*, *98*, 9885–9907.

Rubin, A. M., and J.-P. Ampuero (2005), Earthquake nucleation on (aging) rate and state faults, *J. Geophys. Res.*, *110*, B11312, doi:10.1029/2005JB003686.

Ruina, A. L. (1980), Friction laws and instabilities: A quasistatic analysis of some dry frictional behavior, Ph.D. thesis, Brown Univ., Providence, R. I.

Ruina, A. (1983), Slip instability and state variable friction laws, *J. Geophys. Res.*, *88*, 10,359–10,370.

Schaff, D. P., G. C. Beroza, and B. E. Shaw (1998), Postseismic response of repeating aftershocks, *Geophys. Res. Lett.*, *25*, 4549–4552.

Tse, S. T., and J. R. Rice (1986), Crustal earthquake instability in relation to the depth variation of frictional slip properties, *J. Geophys. Res.*, *91*, 9452–9472.

Toda, S., and R. S. Stein (2002), Response of the San Andreas fault to the 1983 Coalinga-Nuñez earthquakes: An application of interaction-based probabilities for Parkfield, *J. Geophys. Res.*, *107*(B6), 2126, doi:10.1029/2001JB000172.

Vidale, J. E., W. L. Ellsworth, A. Cole, and C. Marone (1994), Variations in rupture process with recurrence interval in a repeated small earthquake, *Nature*, *368*, 624–626.

————————————

A. Ziv, Department of Geological and Environmental Sciences, Ben-Gurion University of the Negev, Mailbox 653, Beer-Sheva 84105, Israel. (zival@bgu.ac.il)